Hyperspectral Methods in Microscopy Image Analysis: A Survey

Shirin Nasr-Esfahani[1][a], Venkatesan Muthukumar[2], Emma E. Regentova[2], Kazem Taghva[1] and Mohamed B. Trabia[3]

[1]*Department of Computer Science, University of Nevada, Las Vegas, U.S.A.*

[2]*Department of Electrical and Computer Engineering, University of Nevada, Las Vegas, U.S.A.*

[3]*Department of Mechanical Engineering, University of Nevada, Las Vegas, U.S.A.*

Keywords: Biology, Confocal, Dark-field, Fluorescence, Hyperspectral Microscope Imaging (HMI), Medicine.

Abstract: Hyperspectral imaging (HSI) has found applications in remote sensing, agriculture, medicine, and biology. HSI acquires a three-dimensional dataset called hypercube, with two spatial dimensions and one spectral dimension. Hyperspectral microscope imaging (HMI) is an emerging imaging spectroscopy technology, which combines the advantages of HSI with microscopic imaging; HSI provides rapid, nondestructive, and chemical free data analysis, whereas a microscope can be used to study microstructure of a sample such as nanoparticles. Integration of HSI and microscopy, results in nondestructive evaluation using both spatial and spectral information along with analysis at the molecular or cellular level. The aim of the survey is an overview of the recent applications for HMI in medicine and biology fields.

1 INTRODUCTION

Microscopic image processing has been an essential part of advancements and discoveries in biology, chemistry, medicine, and other related fields. One example is successful completion of the human genome sequencing project (Wu et al., 2008). It plays a critical role in cancer diagnosis and prognosis processing large amount of image data that when processed manually could be nor accurate and even impossible (time-lapse cell tracking) to process manually.

Hyperspectral imaging (HSI) has been known and widely utilized for many years as a rapid nondestructive technique. It is based on acquiring for every spatial pixel spectral responses in more than a hundred contiguous spectral bands, in a single observation, from the visible and near-infrared, infrared, mid-infrared, and thermal infrared regions of the electromagnetic spectrum (from 400nm up to 100μ m). Henceforth, the hyperspectral technology has been implemented in various fields including remote sensing, food and agriculture, medical science, art, history, forensic science and document processing. Comparing with monochrome or RGB images which have only one- (Figure 1) or three-color channels (Figure 2), hyperspectral images can have several hundred spectral bands. A hyperspectral image denotes a 3D cube, where height and width are considered as two spatial dimensions, and λ (the number of spectral bands) represents the spectral dimension (Figure 3).

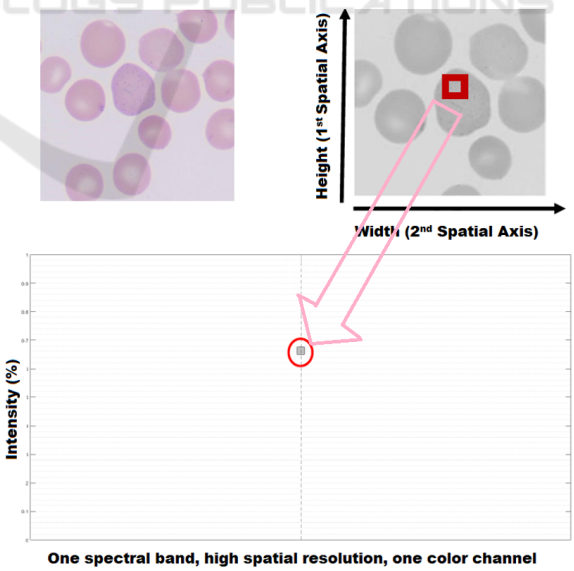

Figure 1: top left: color image, top right: monochrome image, bottom : intensity diagram.

Recently, hyperspectral microscopy is emerging as a powerful technology that has found many

[a] https://orcid.org/0000-0002-8260-1592

Nasr-Esfahani, S., Muthukumar, V., Regentova, E., Taghva, K. and Trabia, M.
Hyperspectral Methods in Microscopy Image Analysis: A Survey.
DOI: 10.5220/0010646701110119
In *Proceedings of the 18th International Conference on Signal Processing and Multimedia Applications (SIGMAP 2021)*, pages 111-119
ISBN: 978-989-758-525-8

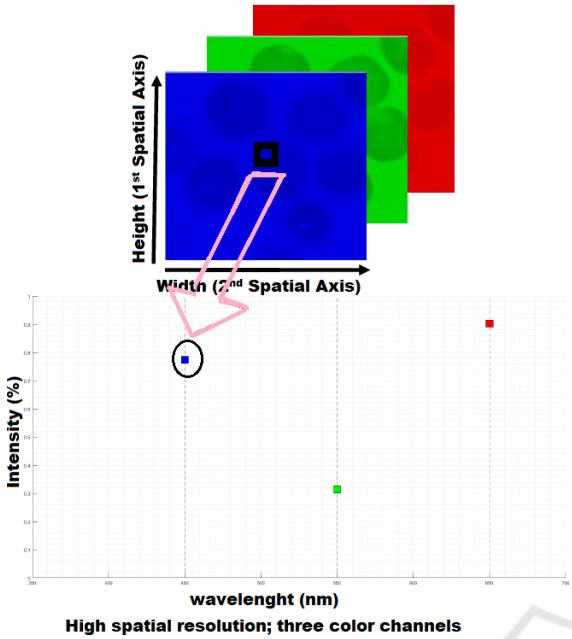

Figure 2: top: RGB data cube, bottom: intensity diagram.

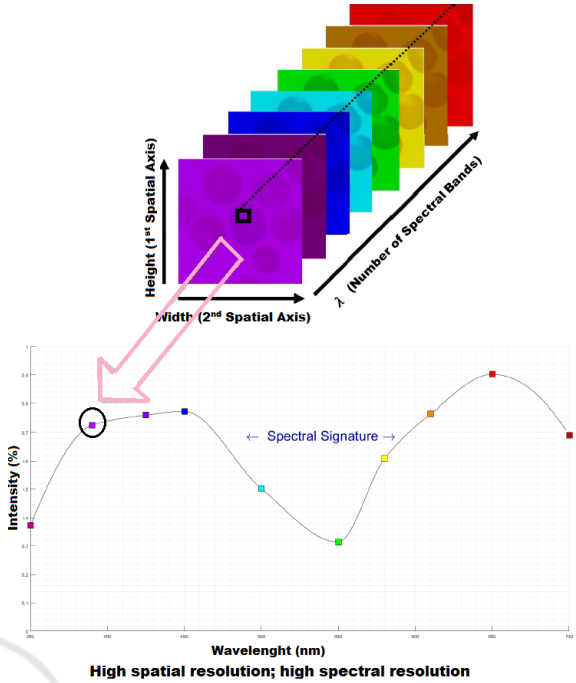

Figure 3: top: hyperspectral data cube, bottom: spectral signature.

biomedical and other applications including disease diagnosis, nanotechnology research, microorganism detection, microscopic contaminants analysis. It is the result of combining conventional microscope systems and spectroscopy technology to collect both high spatial and spectral information. Although being very similar to conventional optical microscope images, HSI microscope images have the complete reflectance spectral response for each pixel in the spatial domain which enables non-destructive measurements. The first development of a hyperspectral microscope imaging system, integration of an imaging spectrometer and an epifluorescence microscope, was used to classify spleen cells of a Balb/c mouse, (Tsurui et al., 1999). Two years later, by combining a standard epifluorescence microscope and an imaging spectrograph, (Schultz et al., 2001) developed a prototype of a hyperspectral imaging microscope to capture and identify a complete emission spectrum from a microscope slide, during a single-pass evaluation.The major problem of both above-mentioned systems was their small fields of view. To solve this issue, (Constantinou et al., 2009) integrated a confocal scanning microscope with a prototype hyperspectral imager to capture the entire slide image. Since then, an extensive research and development has been conducted on HSI microscope technology. The use of machine learning for generating, manipulating, and analysis of high volumes of data at faster rate, has advanced the technology significantly.

The purpose of this paper is to provide a summary of research on the subject in recent years (2016 -2021). HMI instruments are presented in section 2. Application areas of the HMI in medicine and biology fields are discussed in section 3, and section 4 concludes the paper. Finally, all acronyms used in this manual are listed in the Appendix.

2 INSTRUMENTS

A typical HMI system consists of two parts: the optical and the mechanical subsystems. The optical subsystem includes: (1) hyperspectral camera and (2) a microscope, while the mechanical section is composed of (3) a controller of the mechanical system and (4) a stepper motor for stage movement control (Figure 4). Point scanning, and line scanning are among major methods for acquiring hyperspectral images. A point scanning hyperspectral camera can measure a spectrum for each pixel at a time. To construct a whole image, the sample should be re-positioned in both x and y direction. The hyperspectral camera shown in figure 4, is an example of point-scan imager that the stage can move in both X and Y directions (horizontal directions). A line-scan imager collects data, one vertical line at a time. The stage movement is only in one direction (left to right or right to left).

To create two spatial dimensions, multiple lines are assembled to form a complete image. The stepper motor electronically controls stage's movement.

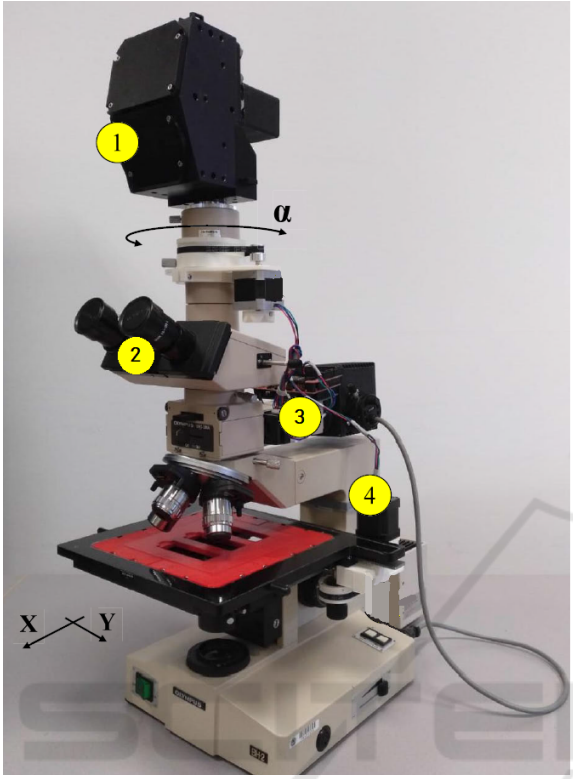

Figure 4: The microscopic hyperspectral imaging system (Ortega et al., 2019).

A microscope can acquire information about the microstructure of a sample. Microscope types used with HMI technology are fluorescence, confocal, and dark field.

The fluorescence microscopy uses the fact that light incident on molecule is absorbed and then emitted in a different color, a process known as fluorescence. Being more sensitive, fluorescence microscopes have gained several advantages over the reflected or transmitted ones. Often, it is possible to attach fluorescent molecules to specific parts of the specimen, making them the only visible ones in the microscope .

The confocal microscope acts like a fluorescence microscope, but instead of illuminating the whole sample at the same time, it illuminates by passing light through a defined point at specific depth, and thus produces high resolution 3D images of the sample (Semwogerere and Weeks, 2005).

Dark-field microscope has the advantage of being a background-free which provides high sensitivity and a large signal-to-noise ratio. The un-scattered light path and its reflection from the surface is excluded from the angular range of signal detection, which causes flat surfaces to appear dark. This technology is usually utilized in imaging of live and unstained biological samples. Although producing the high quality images, dark-field microscope provides low light levels seen in the final image. Therefore, the sample must be very strongly illuminated which can damage the specimen (Harutyunyan et al., 2010).

3 HMI APPLICATIONS

Combining the advantages of hyperspectral technology with microscopic imaging, the two past decades have witnessed a growth of research interest in HMI technology in numerous areas. Unlike conventional microscope images, HMIs have a high spectral resolution which enables them to provide rapid, non-destructive, and chemical-free evaluation methods. This section briefly highlights applications of HMI in medicine and biology.

3.1 Medicine

The HMI has been the fastest-growing and of a high-demand in the medicine field where it has emerged as a potential tool for non-invasive and accurate disease diagnosis as well as treatment monitoring. It is often utilized for various tasks, including object identification or detection, visualization, classification, and feature extraction or measurement.

To increases the chances of survival of patients, early diagnosis of a fatal disease is an essential key to treat it. For example, many cancer types can be treated with a high chance of cure at early stages, but late diagnosis makes the treatment difficult or impossible. To overcome the difficulties of traditional inspection, automated visual inspection systems can assist in identifying suspicious region in real-time that can significantly increase the precision as well as the treatment's accuracy. HMI systems have shown their potential as an alternative imaging technology in identification or detection cells or tissues with high sensitivity and specificity.

Table 1 summarizes various implemented application examples, in terms of image data (organs/specimens), spectral range measured in nanometer (nm), spatial resolution (RES) in micrometer (μm), microscope type, and research achievement.

Although pathology diagnosis is important, conventional methods of pathology analysis important for diagnosis, usually require numerous laborious, time consuming procedures such as freezing, slicing,

Table 1: Summary of key variables for object detection or identification in hyperspectral microscopy images.

Author, Year	Data	Spectral Range	Spatial RES	Micro-scope	Achievement
(Ben Ami et al., 2016)	RPE	420-720	-	fluo-rescence	retinal health & disease investigation
(Leavesley et al., 2016)	colore-ctal tissue	390-450	-	fluo-rescence	early cancer detection
(Seo et al., 2016)	five Staphy lococcus species	450 - 800	-	dark field	Staphy lococcus species identification
(Wang et al., 2016)	cervical tissue	500 - 900	6.43	fluo-rescence	early cancer detection (cellular& tissue)
(Graus et al., 2017)	peri-pheral blood	500 – 850	-	fluo-rescence	Candida species early& accu-rate identification
(Michael et al., 2017)	mouse brain tissue	-	0.47	fluo-rescence	early Alzheimer detection
(Nyström et al., 2017)	mouse brain tissue	490 - 586	-	confocal	Amyloid deposits detection in tissue
(Palombo et al., 2018)	transge-nic mouse brain tissue	-	2 - 8	confocal	early Alzheimer detection
(Wang et al., 2018)	rat_bile duct carci-noma	550 - 1000	-	-	liver tumor analysis
(Yuan et al., 2018)	colon tissue	400 - 1000	6450	-	early cancer detection
(Mahbub et al., 2019)	articular cartilage tissue	400 - 900	-	fluo-rescence	treatment effects detection
(Paugh et al., 2019)	eyelid tissue expressed human meibum	2800-3050 (cm^{-}1)	0.46	fluo-rescence	protein lipid compositional detection
(Song et al., 2019)	ALK P/N lung cancer tissue	550 - 1000	3	-	early lung cancer detection
(Wei et al., 2019)	renal biopsy tissue	400 - 1000	-	fluo-rescence	membranous nephropathy detection
(Liu et al., 2020)	mouse's ear skin	400 - 720	6	photo-acoustic	early stage cutaneous cancers detection
(Laimer et al., 2021)	FFPE tissue	450-900	0.116	fluo-rescence	amalgam tattoos&other pigmented in-traoral lesions identification
(Liu et al., 2021)	normal hepatic & hepatic carcinomas tis-sue	450-720	-	fluo-rescence	hepatic carcinoma cells identification

hematoxylin and eosin staining, and manual analysis which makes the diagnostic procedure much harder. While healthy and normal cells or tissues are generally easier to distinguish, differentiating benign and malignant ones is challenging. The accurate differentiation depends on the experience of the histological specialist. For example, to avoid unnecessary tissue resection during surgery, tumor margins need to be determined precisely. To reduce this burden, non-invasive, rapid, and image-based classification system are highly demanded. A microscope paired with hyperspectral imaging (HSI), has been shown to provide significant performance and promising results for classification task.

Table 2 summarizes examples of classification models, with key information on features.

Table 2: Summary of key variables of hyperspectral microscopy images classification.

Author, Year	Data	Spectral Range	Spatial RES	Micro-scope	Classification Achievement
(Deal et al., 2016)	Sprague Dawley rat	360-600	-	fluo-rescence	hepatic carci-noma cells
(Thatcher et al., 2016)	skin tissue	400-1000	1-10	fluo-rescence	burn injuries skin
(Alfonso-García et al., 2017)	pooled meibum	2800 -3050 (cm^{-}1)	0.46	fluo-rescence	human expressed meibum spec-tral reference
(Bertani et al., 2017)	PBMC	500-1000	1.95	epifluo-rescence	M1/M2 polar-ized human macrophages
(Chen et al., 2019)	human ovarian cells	470-900	-	fluo-rescence	live& dead human ovar-ian cancer cells

Table 2: Summary of key variables of hyperspectral microscopy images classification (cont.).

Author, Year	Data	Spectral Range	Spatial RES	Micro-scope	Classification Achievement
(Duan et al., 2019)	blood cells	-	-	-	Leukocyte
(Ogi et al., 2019)	human neural stem cells	470-900	3.65	-	neuronal cells
(Septiana et al., 2019)	human pancreas tissue	350-1100	-	optical	elastic & collagen fibers
(Bengs et al., 2020)	suspicious &healthy area multi-spectral endoscopic videos	430-680	-	optical	in-vivo head & neck tumor type
(de Lucena et al., 2020)	epithelial tissue	900-2500	1900	-	skin tumor
(Huang et al., 2020)	blood cells	400-720	-	-	blood cells
(Wang et al., 2020a)	HCC biopsy	400-720	-	multi-photon	HCC
(Lv et al., 2021)	renal biopsy tissue	400-1000	-	optical	Membranous Nephropathy
(Sun et al., 2021)	bile duct tissue	550-1000	-	-	CC

The HSI has the advantage of acquiring spectrally encoded information that can be utilized for disease diagnosis purposes and surgery guidance in different ways, such as contrast enhancement for visualization or segmentation tasks, and virtually staining a tissue or an organ without any chemical involvement.

The summary of the related studies is presented in Table 3.

Extracting valuable information in medical images to identify the hidden pattern or subtle relationship is a valuable task that leads to special medical knowledge discovery that is critical to the accuracy of diagnosis and treatment. Hyperspectral imaging technology is a promising technology to assist in feature extraction and measurement tasks.

Relevant studies are reviewed in Table 4.

Table 3: Summary of key variables in hyperspectral microscopic data visualization.

Author, Year	Data	Spectral Range	Spatial RES	Micro-scope	Achievement
(Lin et al., 2016)	Phantom & ex-vivo tissue	-	-	-	tissue surface imaging
(Pichette et al., 2016)	in-vivo brain tissue	480 - 650	5.5	neuro-surgical	brain hemo-dynamic behavior visulaization
(Sen et al., 2016)	in-vivo blood cells & vessels (mouse's retina)	800 - 1000	2	dark field	increasing leukocytes OCT contrast
(Zhang et al., 2016)	H&E stained breast cancer tissue	400 - 700	1.12	lens-free	high resolution ,accurate color reproduction
(Bayramoglu et al., 2017)	mouse lung tissue	500 - 1000	-	-	virtual staining
(Li et al., 2017)	in-vivo retinal tissue (long-Evans)	460 - 630	5.5	commercial	rodent retina color recovery & vessel contrast enhancement

Table 4: Summary of key variables of feature extraction and measurement tasks in hyperspectral microscope images.

Author, Year	Data	Spectral Range	Spatial RES	Micro-scope	Achievement
(Li et al., 2017)	in-vivo retinal tissue (long-Evans)	460 - 630	5.5	comm-ercial	retinal oxygen saturation measurement
(Dey et al., 2019)	ex_vivo retina tissue	400 – 750	-	fluore-scence	autofluorescent substances feature extraction
(Brouwer de Koning et al., 2021)	OSCC	-	-	-	deep_resection oral cancer margin assessment

3.2 Biology

One of the major applications of hyperspectral techniques is within biology that has been found to be effective in matching between spectral signatures and the nature or evolution on many different types of cells. It is also a powerful tool in identification of chemical compositions of complex samples such as cell lysates or bio-fluids. In addition, microscopes are

essential for the analysis of small living organisms, mapping of proteins and genes, or cellular interactions and pathways. Therefore, using hyperspectral imaging methods in combination with microscopy, presents a great potential for biological samples analysis.

Table 5 summarizes recent research achievements in this area.

Table 5: Summery of some biological applications of hyperspectral microscope imaging techniques.

Author, Year	Data	Spectral Range	Spatial RES	Micro-scope	Achievement
(Annamdevula et al., 2016)	- -	420 - 724	-	confocal	3D FRET measurement
(Bradley et al., 2016)	mouse oocytes & pre-implant-ation embryos	> 900	0.1	confocal	quantitative im-ages of lipids in live mouse oocytes & earlyembryos
(Cui et al., 2016)	HeLa, MCF7, SKBR3 cells	300 - 700	5 - 10	dark field	SE-cell optical clearing methodology
(Holzinger et al., 2016)	Chloro-phyta& Charo-phyta	400 - 900	-	epifluo-rescence	different genera determination
(Misra et al., 2016)	-	400 - 1000	-	dark field	prodrug-passivated car-bon nanoparticle synthesis
(Rebner et al., 2016)	peri-pheral lympho-cyte cultures	400 - 1000	-	dark field	characterising unstained human metaphase chromosomes
(Bae et al., 2019)	Staphy lococcus aureus	680 - 1300	0.3125	SRS	interplay be-tween vancomycin & biofilm components dy-namic visualization
(Barnhart-Dailey et al., 2019)	cyano-bacterial	500 - 800	-	confocal	tolyporphins & unusual tetrapyrroles cellular localization
(Fu et al., 2019)	living HeLa cells	200 - 1100	-	selfref-lectance	living cel-lular nano-architecture labelfree_CT
(Wang et al., 2020b)	E.coli in LB	400 - 1000	2 - 6	confocal	monitoring Escherichia coli_biofilms formation
(Nahmad-Rohen et al., 2020)	DOPC, SPH & CHOL Ternary mixture	2700-3100 ($cm^{-}1$)	0.1	epifluo-rescence	lipid partitioning in SE planar membrane bilayers visualization
(Farr et al., 2021)	human dermal fibrob-lasts	-	-	SEM	sterilization effect analysis on bio-material surfaces

4 CONCLUSIONS

HMI systems integrate the advantage of conventional spectroscopy imaging and microscopy techniques to provide relevant information of samples at the molecular or cellular level by providing spatial and spectral information simultaneously. Therefore, HMI tools show great potential in nondestructive evaluation as well as object identification or classification. However, microscopic image analysis is a laborious and error-prone task that is too complex to be performed manually.

Despite the above achievements, there are still many challenges to be overcome in order to to utilize the full potential of HMI in biomedical applications. Data collection is one of the major challenges. In addition, models established based on a certain HMI system cannot be easily adopted by another one. Finally, HMI technology is more expensive than other conventional equipments due to its high spatial and spectral resolutions

The presented survey summarizes the key features of HMIs systems and their applications in medical and biology fields. The analysis of the research work demonstrates that HMI has broad applications ranging from laboratory tasks to clinical studies, yet the future research is still needed to make this technology more efficient and accessible.

REFERENCES

Alfonso-García, A., Paugh, J., Farid, M., Garg, S., Jester, J., and Potma, E. (2017). A machine learning framework to analyze hyperspectral stimulated Raman scattering microscopy images of expressed human meibum: HsSRS microscopy and machine learning analysis of human meibum. *Journal of Raman Spectroscopy*, 48(6):803–812.

Annamdevula, N. S., Sweat, R., Britain, A., Rich, T. C., and Leavesley, S. J. (2016). Hyperspectral Imaging

Approaches for Measuring Three-Dimensional FRET. *The FASEB Journal*, 30(S1):969.27–969.27.

Bae, K., Zheng, W., Ma, Y., and Huang, Z. (2019). Real-Time Monitoring of Pharmacokinetics of Antibiotics in Biofilms with Raman-Tagged Hyperspectral Stimulated Raman Scattering Microscopy. *Theranostics*, 9(5):1348–1357.

Barnhart-Dailey, M., Zhang, Y., Zhang, R., Anthony, S. M., Aaron, J. S., Miller, E. S., Lindsey, J. S., and Timlin, J. A. (2019). Cellular localization of tolyporphins, unusual tetrapyrroles, in a microbial photosynthetic community determined using hyperspectral confocal fluorescence microscopy. *Photosynthesis Research*, 141(3):259–271.

Bayramoglu, N., Kaakinen, M., Eklund, L., and Heikkila, J. (2017). Towards Virtual H&E Staining of Hyperspectral Lung Histology Images Using Conditional Generative Adversarial Networks. In *2017 IEEE International Conference on Computer Vision Workshops (ICCVW)*, pages 64–71, Venice, Italy. IEEE.

Ben Ami, T., Tong, Y., Bhuiyan, A., Huisingh, C., Ablonczy, Z., Ach, T., Curcio, C. A., and Smith, R. T. (2016). Spatial and Spectral Characterization of Human Retinal Pigment Epithelium Fluorophore Families by Ex Vivo Hyperspectral Autofluorescence Imaging. *Translational Vision Science & Technology*, 5(3):5.

Bengs, M., Gessert, N., Laffers, W., Eggert, D., Westermann, S., Mueller, N. A., Gerstner, A. O. H., Betz, C., and Schlaefer, A. (2020). Spectral-spatial Recurrent-Convolutional Networks for In-Vivo Hyperspectral Tumor Type Classification. In Martel, A. L., Abolmaesumi, P., Stoyanov, D., Mateus, D., Zuluaga, M. A., Zhou, S. K., Racoceanu, D., and Joskowicz, L., editors, *Medical Image Computing and Computer Assisted Intervention – MICCAI 2020*, volume 12263, pages 690–699. Springer International Publishing, Cham. Series Title: Lecture Notes in Computer Science.

Bertani, F. R., Mozetic, P., Fioramonti, M., Iuliani, M., Ribelli, G., Pantano, F., Santini, D., Tonini, G., Trombetta, M., Businaro, L., Selci, S., and Rainer, A. (2017). Classification of M1/M2-polarized human macrophages by label-free hyperspectral reflectance confocal microscopy and multivariate analysis. *Scientific Reports*, 7(1):8965.

Bradley, J., Pope, I., Masia, F., Sanusi, R., Langbein, W., Swann, K., and Borri, P. (2016). Quantitative imaging of lipids in live mouse oocytes and early embryos using CARS microscopy. *Development*, page dev.129908.

Brouwer de Koning, S. G., Schaeffers, A. W. M. A., Schats, W., van den Brekel, M. W. M., Ruers, T. J. M., and Karakullukcu, M. B. (2021). Assessment of the deep resection margin during oral cancer surgery: A systematic review. *European Journal of Surgical Oncology: The Journal of the European Society of Surgical Oncology and the British Association of Surgical Oncology*.

Chen, H., Ho, B., Wang, H., Tan, S. H., Zhao, C.-X., Nguyen, N.-T., Gao, Y., and Zhou, J. (2019). Automatic Live and Dead Cell Classification via Hyperspectral Imaging. In *2019 10th Workshop on Hyperspectral Imaging and Signal Processing: Evolution in Remote Sensing (WHISPERS)*, pages 1–5, Amsterdam, Netherlands. IEEE.

Constantinou, P., Dacosta, R., and Wilson, B. (2009). Extending immunofluorescence detection limits in whole paraffin-embedded formalin fixed tissues using hyperspectral confocal fluorescence imaging. *Journal of Microscopy*, 234(2):137–146.

Cui, Y., Wang, X., Ren, W., Liu, J., and Irudayaraj, J. (2016). Optical Clearing Delivers Ultrasensitive Hyperspectral Dark-Field Imaging for Single-Cell Evaluation. *ACS Nano*, 10(3):3132–3143.

de Lucena, D. V., da Silva Soares, A., Coelho, C. J., Wastowski, I. J., and Filho, A. R. G. (2020). Detection of Tumoral Epithelial Lesions Using Hyperspectral Imaging and Deep Learning. In Krzhizhanovskaya, V. V., Závodszky, G., Lees, M. H., Dongarra, J. J., Sloot, P. M. A., Brissos, S., and Teixeira, J., editors, *Computational Science – ICCS 2020*, pages 599–612, Cham. Springer International Publishing.

Deal, J. A., Favreau, P., Weber, D., Rich, T., and Leavesley, S. (2016). Potential of Hyperspectral Imaging for Label-free Tissue and Pathology Classification. *The FASEB Journal*, 30(S1).

Dey, N., Hong, S., Ach, T., Koutalos, Y., Curcio, C. A., Smith, R. T., and Gerig, G. (2019). Tensor decomposition of hyperspectral images to study autofluorescence in age-related macular degeneration. *Medical Image Analysis*, 56:96–109.

Duan, Y., Wang, J., Hu, M., Zhou, M., Li, Q., Sun, L., Qiu, S., and Wang, Y. (2019). Leukocyte classification based on spatial and spectral features of microscopic hyperspectral images. *Optics & Laser Technology*, 112:530–538.

Farr, N., Thanarak, J., Schäfer, J., Quade, A., Claeyssens, F., Green, N., and Rodenburg, C. (2021). Understanding Surface Modifications Induced via Argon Plasma Treatment through Secondary Electron Hyperspectral Imaging. *Advanced Science*, 8(4):2003762.

Fu, R., Su, Y., Wang, R., Lin, X., Jiang, K., Jin, X., Yang, H., Ma, L., Luo, X., Lu, Y., and Huang, G. (2019). Label-free tomography of living cellular nanoarchitecture using hyperspectral self-interference microscopy. *Biomedical Optics Express*, 10(6):2757.

Graus, M. S., Neumann, A. K., and Timlin, J. A. (2017). Hyperspectral fluorescence microscopy detects autofluorescent factors that can be exploited as a diagnostic method for *Candida* species differentiation. *Journal of Biomedical Optics*, 22(1):016002.

Harutyunyan, H., Palomba, S., Renger, J., Quidant, R., and Novotny, L. (2010). Nonlinear Dark-Field Microscopy. *Nano Letters*, 10(12):5076–5079. Publisher: American Chemical Society.

Holzinger, A., Allen, M. C., and Deheyn, D. D. (2016). Hyperspectral imaging of snow algae and green algae from aeroterrestrial habitats. *Journal of Photochemistry and Photobiology B: Biology*, 162:412–420.

Huang, Q., Li, W., Zhang, B., Li, Q., Tao, R., and Lovell, N. H. (2020). Blood Cell Classification Based on Hyperspectral Imaging With Modulated Gabor and CNN.

IEEE Journal of Biomedical and Health Informatics, 24(1):160–170.

Laimer, J., Bruckmoser, E., Helten, T., Kofler, B., Zelger, B., Brunner, A., Zelger, B., Huck, C. W., Tappert, M., Rogge, D., Schirmer, M., and Pallua, J. D. (2021). Hyperspectral imaging as a diagnostic tool to differentiate between amalgam tattoos and other dark pigmented intraoral lesions. *Journal of Biophotonics*, 14(2).

Leavesley, S. J., Walters, M., Lopez, C., Baker, T., Favreau, P. F., Rich, T. C., Rider, P. F., and Boudreaux, C. W. (2016). Hyperspectral imaging fluorescence excitation scanning for colon cancer detection. *Journal of Biomedical Optics*, 21(10):104003.

Li, H., Liu, W., Dong, B., Kaluzny, J. V., Fawzi, A. A., and Zhang, H. F. (2017). Snapshot hyperspectral retinal imaging using compact spectral resolving detector array. *Journal of Biophotonics*, 10(6-7):830–839.

Lin, J., Clancy, N. T., Sun, X., Qi, J., Janatka, M., Stoyanov, D., and Elson, D. S. (2016). Probe-Based Rapid Hybrid Hyperspectral and Tissue Surface Imaging Aided by Fully Convolutional Networks. In Ourselin, S., Joskowicz, L., Sabuncu, M. R., Unal, G., and Wells, W., editors, *Medical Image Computing and Computer-Assisted Intervention - MICCAI 2016*, volume 9902, pages 414–422. Springer International Publishing, Cham. Series Title: Lecture Notes in Computer Science.

Liu, K., Lin, S., Zhu, S., Chen, Y., Yin, H., Li, Z., and Chen, Z. (2021). Hyperspectral microscopy combined with DAPI staining for the identification of hepatic carcinoma cells. *Biomedical Optics Express*, 12(1):173.

Liu, N., Chen, Z., and Xing, D. (2020). Integrated photoacoustic and hyperspectral dual-modality microscopy for co-imaging of melanoma and cutaneous squamous cell carcinoma in vivo. *Journal of Biophotonics*, 13(8).

Lv, M., Li, W., Tao, R., and Lovell, N. H. (2021). Spatial-Spectral Density Peaks-Based Discriminant Analysis for Membranous Nephropathy Classification Using Microscopic Hyperspectral Images. *IEEE Journal of Biomedical and Health Informatics*, pages 1–1.

Mahbub, S. B., Guller, A., Campbell, J. M., Anwer, A. G., Gosnell, M. E., Vesey, G., and Goldys, E. M. (2019). Non-Invasive Monitoring of Functional State of Articular Cartilage Tissue with Label-Free Unsupervised Hyperspectral Imaging. *Scientific Reports*, 9(1):4398.

Michael, R., Lenferink, A., Vrensen, G. F. J. M., Gelpi, E., Barraquer, R. I., and Otto, C. (2017). Hyperspectral Raman imaging of neuritic plaques and neurofibrillary tangles in brain tissue from Alzheimer's disease patients. *Scientific Reports*, 7(1):15603.

Misra, S. K., Ostadhossein, F., Daza, E., Johnson, E. V., and Pan, D. (2016). Hyperspectral Imaging Offers Visual and Quantitative Evidence of Drug Release from Zwitterionic-Phospholipid-Nanocarbon When Concurrently Tracked in 3D Intracellular Space. *Advanced Functional Materials*, 26(44):8031–8041.

Nahmad-Rohen, A., Regan, D., Masia, F., McPhee, C., Pope, I., Langbein, W., and Borri, P. (2020). Quantitative Label-Free Imaging of Lipid Domains in Single Bilayers by Hyperspectral Coherent Raman Scattering. *Analytical Chemistry*, 92(21):14657–14666.

Nyström, S., Bäck, M., Nilsson, K. P. R., and Hammarström, P. (2017). Imaging Amyloid Tissues Stained with Luminescent Conjugated Oligothiophenes by Hyperspectral Confocal Microscopy and Fluorescence Lifetime Imaging. *Journal of Visualized Experiments*, (128):56279.

Ogi, H., Moriwaki, S., Kokubo, M., Hikida, Y., and Itoh, K. (2019). Label-free classification of neurons and glia in neural stem cell cultures using a hyperspectral imaging microscopy combined with machine learning. *Scientific Reports*, 9(1):633.

Ortega, S., Guerra, R., Diaz, M., Fabelo, H., Lopez, S., Callico, G. M., and Sarmiento, R. (2019). Hyperspectral Push-Broom Microscope Development and Characterization. *IEEE Access*, 7:122473–122491.

Palombo, F., Masia, F., Mattana, S., Tamagnini, F., Borri, P., Langbein, W., and Fioretto, D. (2018). Hyperspectral analysis applied to micro-Brillouin maps of amyloid-beta plaques in Alzheimer's disease brains. *The Analyst*, 143(24):6095–6102.

Paugh, J. R., Alfonso-Garcia, A., Nguyen, A. L., Suhalim, J. L., Farid, M., Garg, S., Tao, J., Brown, D. J., Potma, E. O., and Jester, J. V. (2019). Characterization of expressed human meibum using hyperspectral stimulated Raman scattering microscopy. *The Ocular Surface*, 17(1):151–159.

Pichette, J., Laurence, A., Angulo, L., Lesage, F., Bouthillier, A., Nguyen, D. K., and Leblond, F. (2016). Intraoperative video-rate hemodynamic response assessment in human cortex using snapshot hyperspectral optical imaging. *Neurophotonics*, 3(04):1.

Rebner, K., Ostertag, E., and Kessler, R. W. (2016). Hyperspectral backscatter imaging: a label-free approach to cytogenetics. *Analytical and Bioanalytical Chemistry*, 408(21):5701–5709.

Schultz, R. A., Nielsen, T., Zavaleta, J. R., Ruch, R., Wyatt, R., and Garner, H. R. (2001). Hyperspectral imaging: A novel approach for microscopic analysis. *Cytometry*, 43(4):239–247.

Semwogerere, D. and Weeks, E. R. (2005). *G. Wnek, G. Bowlin (Eds.), Encyclopedia of Biomaterials and Biomedical Engineerin*. Taylor and Francis, New York.

Sen, D., SoRelle, E. D., Liba, O., Dalal, R., Paulus, Y. M., Kim, T.-W., Moshfeghi, D. M., and de la Zerda, A. (2016). High-resolution contrast-enhanced optical coherence tomography in mice retinae. *Journal of Biomedical Optics*, 21(06):1.

Seo, Y., Park, B., Hinton, A., Yoon, S.-C., and Lawrence, K. C. (2016). Identification of Staphylococcus species with hyperspectral microscope imaging and classification algorithms. *Journal of Food Measurement and Characterization*, 10(2):253–263.

Septiana, L., Suzuki, H., Ishikawa, M., Obi, T., Kobayashi, N., Ohyama, N., Ichimura, T., Sasaki, A., Wihardjo, E., and Andiani, D. (2019). Elastic and collagen fibers discriminant analysis using H&E stained hyperspectral images. *Optical Review*, 26(4):369–379.

Song, J., Hu, M., Wang, J., Zhou, M., Sun, L., Qiu, S., Li, Q., Sun, Z., and Wang, Y. (2019). ALK positive lung

cancer identification and targeted drugs evaluation using microscopic hyperspectral imaging technique. *Infrared Physics & Technology*, 96:267–275.

Sun, L., Zhou, M., Li, Q., Hu, M., Wen, Y., Zhang, J., Lu, Y., and Chu, J. (2021). Diagnosis of cholangiocarcinoma from microscopic hyperspectral pathological dataset by deep convolution neural networks. *Methods*.

Thatcher, J. E., Squiers, J. J., Kanick, S. C., King, D. R., Lu, Y., Wang, Y., Mohan, R., Sellke, E. W., and DiMaio, J. M. (2016). Imaging Techniques for Clinical Burn Assessment with a Focus on Multispectral Imaging. *Advances in Wound Care*, 5(8):360–378.

Tsurui, H., Lerner, J. M., Takahashi, K., Hirose, S., Mitsui, K., Okumura, K., and Shirai, T. (1999). Hyperspectral imaging of pathology samples. pages 273–281, San Jose, CA.

Wang, C., Zheng, W., Bu, Y., Chang, S., Zhang, S., and Xu, R. X. (2016). Multi-scale hyperspectral imaging of cervical neoplasia. *Archives of Gynecology and Obstetrics*, 293(6):1309–1317.

Wang, J., Hu, M., Zhou, M., Sun, L., and Li, Q. (2018). Segmentation of Pathological Features of Rat Bile Duct Carcinoma from Hyperspectral Images. In *2018 11th International Congress on Image and Signal Processing, BioMedical Engineering and Informatics (CISP-BMEI)*, pages 1–5, Beijing, China. IEEE.

Wang, R., He, Y., Yao, C., Wang, S., Xue, Y., Zhang, Z., Wang, J., and Liu, X. (2020a). Classification and Segmentation of Hyperspectral Data of Hepatocellular Carcinoma Samples Using 1-D Convolutional Neural Network. *Cytometry Part A*, 97(1):31–38.

Wang, Y., Reardon, C. P., Read, N., Thorpe, S., Evans, A., Todd, N., Van Der Woude, M., and Krauss, T. F. (2020b). Attachment and antibiotic response of early-stage biofilms studied using resonant hyperspectral imaging. *npj Biofilms and Microbiomes*, 6(1):57.

Wei, X., Tu, T., Zhang, N., Yang, Y., Li, W., and Li, W. (2019). Membranous Nephropathy Identification Using Hyperspectral Microscopic Images. In Lin, Z., Wang, L., Yang, J., Shi, G., Tan, T., Zheng, N., Chen, X., and Zhang, Y., editors, *Pattern Recognition and Computer Vision*, pages 173–184, Cham. Springer International Publishing.

Wu, Q., Merchant, F. A., and Castleman, K. R., editors (2008). *Microscope image processing*. Elsevier/Academic Press, Amsterdam ; Boston.

Yuan, X., Zhang, D., Wang, C., Dai, B., Zhao, M., and Li, B. (2018). Hyperspectral Imaging and SPA–LDA Quantitative Analysis for Detection of Colon Cancer Tissue. *Journal of Applied Spectroscopy*, 85(2):307–312.

Zhang, Y., Wu, Y., Zhang, Y., and Ozcan, A. (2016). Color calibration and fusion of lens-free and mobile-phone microscopy images for high-resolution and accurate color reproduction. *Scientific Reports*, 6(1):27811.

APPENDIX

Acronyms

AMD age-related macular degeneration

CC cholangiocarcinoma

CT computed tomography

CHOL cholesterol

E.coli escherichia coli

DOPC dioleoylphosphatidylcholine

FFPE formalin-fixed paraffin-embedded

FRET förster resonance energy transfer

H&E hematoxylin and eosin stain

HCC hepatocellular carcinoma

HeLa henrietta lacks

HMI hyperspectral microscope imaging

HSI hyperspectral imaging

LB luria-bertani

MCF7 Michigan cancer foundation-7

OCT optical coherence tomography

OSCC oral squamous cell carcinoma

PBMC peripheral blood mononuclear cells

P/N positive and negative

RES resolution

RPE retinal pigment epithelium

SEM scanning electron microscope

SE single

SRS stimulated raman scatering

SPH sphingomyelin

TP tolyporphins